

EFFECT OF ROTATION BEHAVIOR ON MECHANICAL PROPERTIES OF MULTI-CELL TYPE NATURAL FIBRE

Y. Nitta¹, K. Goda²

¹Department of Mechanical Engineering, National Institute of Technology, Ube College, 2-14-1 Tokiwadai, Ube, Yamaguchi, 755-8555, Japan

Email: nitta@ube-k.ac.jp, Web Page: <http://www.ube-k.ac.jp/en/>

²Department of Mechanical Engineering, Yamaguchi University, 2-16-1, Tokiwadai, Ube, Yamaguchi, 755-8611, Japan

Email: goda@yamaguchi-u.ac.jp, Web Page: <http://www.gse.yamaguchi-u.ac.jp/EN/>

Keywords: Kenaf fibre, Multi-cell structure, Tensile strength, Rotation, FEM

Abstract

The purpose of this study is to find a rotation phenomenon around the fibre axis of a kenaf fibre, a representative multi-cell type fibre, during tensile loading, and clarify the relation between rotation behavior and fibre mechanical properties. Results showed that, although many fibre specimens did not rotate during tensile loading, the rotation was confirmed for approximately one fourth of all the specimens. Rotation identified fibres indicated a slight decrease in strength, as compared with non-rotating fibres. Furthermore, to clarify rotation mechanism of multi-cell type natural fibres, a 3D finite element model was constructed in which spiral structure of cellulose microfibrils (CMF) was taken into account. As a result, rotation phenomenon was estimated to be caused by the helical structure of CMF. Moreover, the influence of variation in microfibrillar angle on Young's modulus was explored for a single cell fibre using the finite element model.

1. Introduction

Nowadays, global environmental problems about CO₂ emission become serious concerns, and therefore a number of biomass-based material researches are being increased. Natural fibres, such as flax, ramie and kenaf, are often used as reinforcement of natural fibre composites. These composites is expected for practical use as unidirectional composites and injection-molded material . In general, plant-based natural fibres is composed of single elementary fibre in many cells. Cellulose microfibrils (hereinafter, referred to CMF) in the cell of natural fibre are helically oriented in the cell axis. The orientation angle of CMF called 'microfibrillar angle' (hereinafter, referred to MFA) is often said such that it is important parameter to influence mechanical properties of natural fibres [1, 2]. Relationship between MFA and mechanical property have been discussed based on natural fibre consisting of one cell (hereinafter, referred to as 'single cell' fibres) [3]. Recently, it is also discussed about natural fibres consisting of many cells (Hereinafter, referred to as 'multi-cell' fibres) [4, 5].

On the other hand, rotation during swelling or tensile loading has been identified as specific phenomenon of plant-based natural fibres [3, 6, 7]. It is considered that rotation is caused by helical orientation of the cellulose microfibrils. The mechanism of this phenomenon has been discussed in the basis of the structure of a single-cell fibre as in the above references [3, 6, 7], but not been done from the viewpoint of the multi-cell structure.

The purpose of this study is thus to investigate the effect of rotation behaviour on mechanical properties by single fibre test using a kenaf fibre, one of the representative multi-cell fibres. The rotation phenomenon of a multi-cell type fibre is also discussed using a 3D finite element model. Furthermore, the influence of statistical variation in MFA on Young's modulus was also investigated using the 3D-FEM.

2. Experiment method

Natural fibre used in experiment is a kenaf fibre (*Hibiscus cannabinus*), one of typical multi-cell fibres. A typical kenaf fibre cross-section is shown in Fig.1. Single fibre tensile test was carried out using a tension and compression testing machine produced in Yamaguchi University, to which a 20N load cell was attached. The gauge length of the tensile specimen was 25 mm, the tensile speed was 1.0 mm/min and the number of samples was forty two. The projective widths of the specimen were measured from three directions of 0, 60 and 120 degrees at 0.1 mm interval along its axial direction, using a laser scan micro-meter (LSM-500S, Mitutoyo Corporation, Japan). The fibre cross-sectional area was then estimated using DBA (Data-based approximation) method [8, 9]. In this study, the shape of cross-section was assumed as a hexagon. Displacement during tensile test was measured using a laser displacement meter (KEYENCE, LS-7500, Japan), and changed to nominal strain. Finally, the stress-strain diagram was made for each specimen, and Young's modulus was calculated based on a linear strain interval of 0.2% in the range of 0.2% to 0.6% strain. In this study, one of the specimen's gripping jigs was designed as a *free* condition at the rotation direction. The upper jig was linked with a metal ring, which was supported by a metal rod. The ring can therefore turn within the range less than ± 90 degree rotation angle. Thus, the fiber specimen can rotate around the fiber axis, if any rotating mechanism works inside the fiber during tensile test. Fibre rotation angle was measured during tensile test from motion images, which were photographed by a digital microscope (KH-1300, HiROX). Rotation angle was determined from the following equation as :

$$L = x_0 - x_0 \cos \psi + y_0 \sin \psi \quad (1)$$

where, L , x_0 and y_0 are the measured distance of movement path, and the position coordinates of the initial feature point, respectively. In this study, the origin was recognized as the cross point of three diagonal lines in an assumed hexagon [8], derived from DBA, and y_0 was assumed as a point on a side of the hexagon. Rotation angle was obtained by solving eq. (1) by an implicit method.

3. Experimental result

Figure 2 shows the fibre surface during tensile test. The feature point, as shown in the arrow, moves to the left (Fig. 2(a)) from the right (Fig. 2(c)), as well as movement to the upper side. Fibre rotation of Fig. 2 is anticlockwise at the top view. It is also observed in Fig. 2 that the fibre width changes with rotation because kenaf fibre cross-section exhibits a complicated shape. On the other hand, some

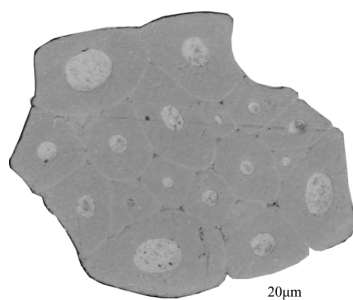


Figure 1. Typical cross-section of a kenaf fibre.

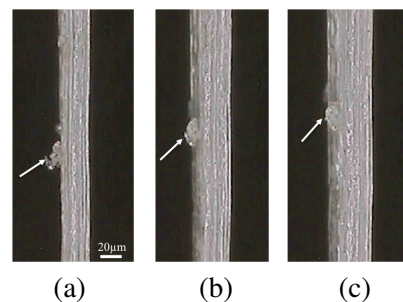


Figure 2. Rotation of a kenaf fibre during tensile test.

Table 1. Tensile properties of kenaf fibre specimens.

	Corresponding number	Tensile strength (MPa)	Young's modulus (GPa)
Total	42	350 (0.331)	33.0 (0.303)
RI specimens	11	331 (0.266)	32.8 (0.330)
NRI specimens	31	357 (0.347)	33.1 (0.293)

The values in parentheses are coefficients of variation. NRI: non-rotation identified.

specimens rotated clockwise. But, as been in Table 1, many specimens did not rotate in this study.

Table 1 shows the results of tensile test of the specimen. The total number of specimens was 42, but rotation identified specimens (hereinafter, this is denoted as 'RI-specimen') and were only eleven, about one fourth of all. Rotation angle of specimens was able to be measured for nine specimens. Tensile strength of RI-specimens decreases slightly, as compared with the result of all specimens, but their difference is not so significant. Young's modulus of RI-specimens is also even, as compared to that of the all specimens. If the rotation behavior is attributed to the internal structure of the multi-cell fibre, strength of plant-based natural fibre would be sensitive to structure. And also we would say that stiffness is almost insensitive to the structure. The correlation coefficient of between tensile strength and rotation angle was calculated as -0.211. On the other hand, the correlation coefficient between Young's modulus and rotation was -0.518. This value is accepted as a mild correlation between both of them. However, the coefficient values obtained in this study is not sufficiently reliable, because these are estimated only from nine data. Relation of strength and stiffness to rotation angle of the specimens requires further investigation as a future issue. Thus, the rotation mechanism of the multi-cell fibre is discussed from the viewpoint of simulational approach using 3D-FEM.

4. Discussion

4.1. 3D-FEM method

As mentioned above, fibre rotation was observed during a single fibre tensile test. This mechanism is considered as follows: CMF is spirally placed around the cell axis. MFA is reduced during tensile loading, which results in fibre rotation. However, in multi-cell type fibres, elementary cells are mutually bonded at inter-cells through substances such as lignin and pectin. Thus, verification of rotation mechanism needs some mechanical modeling. From such point of view, we decided to make a longitudinally arranged multi-cell model, using 3D-FEM.

The finite element model used here was an isoparametric 8-node hexahedral element. The cross-section of one cell model is assumed as a hexagon with a hole, as shown in Fig. 3(a). The unit cell of Fig. 3(a) was piled up, as shown in Fig. 3(b). Each element was assumed as an orthotropic body, because microfibrils are recognized as a unidirectional fibre bundle. The length of one side of a hexagon was approximated as 0.005mm with reference to the cross-sectional photo of a kenaf fibre, and the longitudinal length of an element was 0.02 mm. In general the stiffness matrix in the stress-strain relation of an orthotropic body is expressed by a transformation matrix. In this study, the transformation matrix [T] to

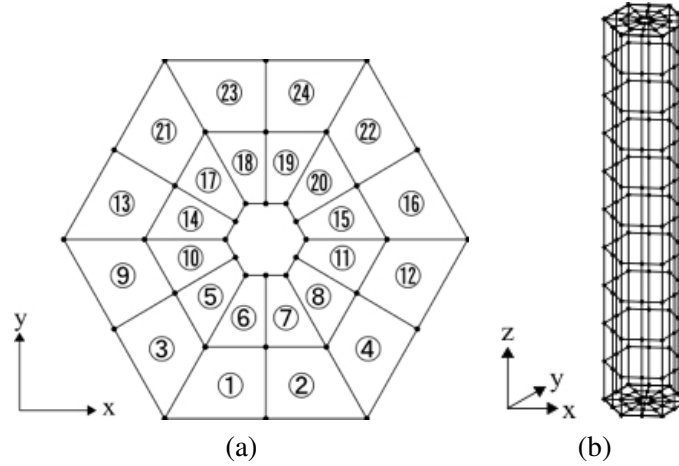


Figure 3. FEM mesh of one elementary cell. (a) Cross-sectional FE mesh, (b) 3D-FE mesh

express MFA was given as:

$$\begin{aligned}
 [T] = & \begin{bmatrix} l^2 & m^2 & n^2 & 2lm & 2mn & 2nl \\ l'^2 & m'^2 & n'^2 & 2l'm' & 2m'n' & 2n'l' \\ l''^2 & m''^2 & n''^2 & 2l''m'' & 2m''n'' & 2n''l'' \\ ll' & mm' & nn' & lm' + l'm & mn' + m'n & nl' + n'l \\ l'l'' & m'm'' & n'n'' & l'm'' + l''m' & m'n'' + m''n' & n'l'' + n''l' \\ ll'' & mm'' & nn'' & lm'' + l''m & mn'' + m''n & nl'' + n''l \end{bmatrix} \quad (2) \\
 l = \cos \phi & \quad m = -\sin \phi \sin \theta \quad n = -\sin \phi \cos \theta \\
 l' = 0 & \quad m' = \cos \theta \quad n' = -\sin \theta \\
 l'' = \sin \phi & \quad m'' = \cos \phi \sin \theta \quad n'' = \cos \phi \cos \theta
 \end{aligned}$$

where, ϕ and θ are rotation angles of x - z and y - z planes, respectively, as shown in Fig. 4. MFA denoted as α , and CMF-axis are given with the angle α from z -axis as shown in the element of Fig. 4, which is perpendicular to the normal line extending to a radial direction on the x - y plane from the origin. As indicated by arrows in Fig. 4, when it is moved toward the origin O , CMF-axis coincides with the vector OR and therefore α is given by the inverse function of $\cos \phi \cos \theta$. ϕ and θ were estimated by assigning β following the coordinates of each element, in order to express MFA spirally around z -axis. Table 2 shows the conversion formula.

The material constants used were given as follows:

$$E_1 = E_2 = 10.0 \text{ GPa}, E_3 = 30.0 \text{ GPa}, G_{12} = G_{23} = G_{31} = 7.0 \text{ GPa}, \nu_{31} = \nu_{32} = 0.2, \nu_{12} = 0.3$$

These constants were assumed based on the present experiment and the references [4, 10, 11]. Nodal-points at the bottom were fixed along the z -axis, and a forced displacement of 0.002mm was given as a boundary condition at the top along the z -axis. Then, helical structure of CMF was assumed as Z -helix[12]. In this study, the tensile direction was only z -axis, and no load was applied along x - and y -axes. In addition, nodal points around the hole in the unit cell at the bottom were fixed along x - and y -axes. The FEM code used in this study is an original program developed by the authors.

4.2. Simulation results

Figure 5 shows the top view of nodal-points position obtained in the one-cell model when $\alpha=10^\circ$. Z -helix is a helical structure of the anticlockwise at the top view, and therefore clockwise rotation is

Table 2. Relation of MFA (α) and location angle β to coordinate transformation angles ϕ, θ

	First quadrant	Second quadrant	Third quadrant	Forth quadrant
ϕ	$\tan^{-1}(\tan \alpha \cos(\pi - \beta))$	$\tan^{-1}(\tan(\pi - \alpha) \cos(\pi + \beta))$	$\tan^{-1}(\tan(\pi - \alpha) \cos(-\beta))$	$\tan^{-1}(\tan \alpha \cos(\beta))$
θ	$\cos^{-1}\left(\frac{\cos \alpha}{\cos \phi}\right)$	$\cos^{-1}\left(-\frac{\cos(\pi - \alpha)}{\cos \phi}\right)$	$\cos^{-1}\left(\frac{\cos(\pi - \alpha)}{\cos \phi}\right)$	$\cos^{-1}\left(-\frac{\cos \alpha}{\cos \phi}\right)$

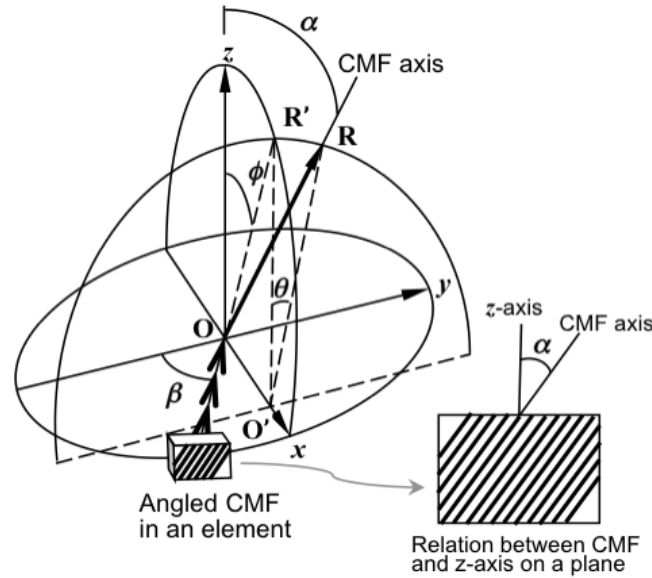


Figure 4. Schematic of coordinates transformation on x - z and y - z planes.

generated by applying a tensile load, as shown in Fig. 5. Rotation angle was 4.89° per 0.2 mm fibre length ($24.5^\circ/\text{mm}$), and Young's modulus of fibre axis direction (off-axis direction) was obtained as 28.6 GPa.

In general, according to orthotropic theory, the off-axis elastic modulus of a lamina, $E(\alpha)$, is given as:

$$E(\alpha) = \left\{ \frac{\cos^4 \alpha}{E_1} + \left(\frac{1}{G_{12}} - \frac{2\nu_{12}}{E_1} \right) \cos^2 \alpha \cdot \sin^2 \alpha + \frac{\sin^4 \alpha}{E_2} \right\}^{-1} \quad (3)$$

where, α is an off-axis angle. By substituting the material constants described in the above into eq. (3), the elastic modulus was calculated as 28.5 GPa. This value is slightly lower than the value, 28.6GPa, obtained in the present FE model. To simulate a multi-cell structure, one-cell model is extended to the model consisting of seven hexagons, as shown in Fig. 6. As a result, clockwise rotation was confirmed similarly to one-cell model as shown in Fig. 7. Rotation angle was obtained as 0.95° ($4.75^\circ/\text{mm}$), although rotation angle is smaller than the one-cell model. This is because microfibrils in the elements at neighboring cells incline each other to the opposite direction. Young's modulus was obtained as 29.1 GPa, this value is larger than that of one-cell model. Young's moduli of one-cell, two-cell and seven-cell models were calculated for various MFA (α), and compared with theoretical off-axis elastic modulus of the lamina. The results are shown in Fig. 8. Every Young's moduli of the present cell models are higher than that of lamina. And, the Young's modulus increases with an increase in the number of cells. From this simulation result, it is considered that less rotation angle of the fibre tend to show higher Young's modulus. In other words, the structure of multi-cell fibres is an advantage point to maintain the stiffness of a natural fibre, even if relatively high MFA is contained. According to the experimental result, on the other hand, the fibres rotated clockwise or anticlockwise. It should also be clarified why the fibre rotates

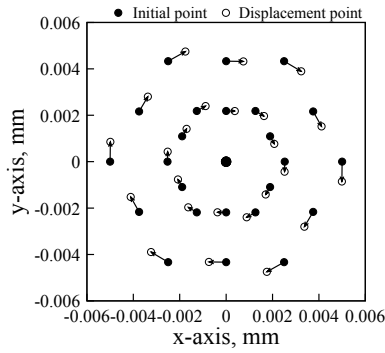


Figure 5. The calculation result of one-cell model at $\alpha = 10^\circ$ (Top view)

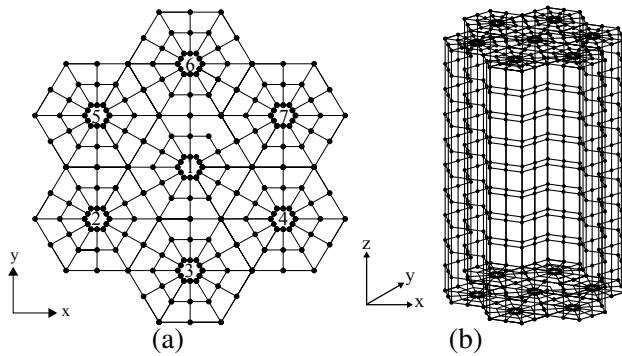


Figure 6. FEM mesh of seven elementary cell. (a) Cross-sectional FE mesh, (b) 3D-FE mesh

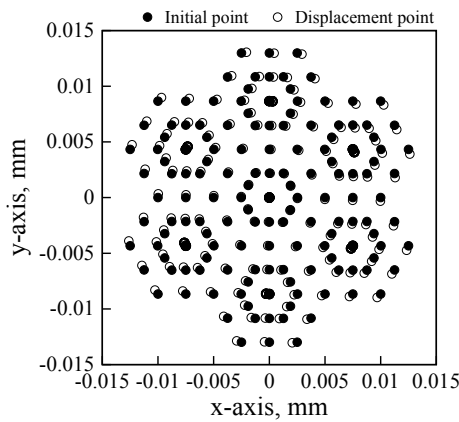


Figure 7. The calculation result of seven-cell model at $\alpha = 10^\circ$ (Top view)

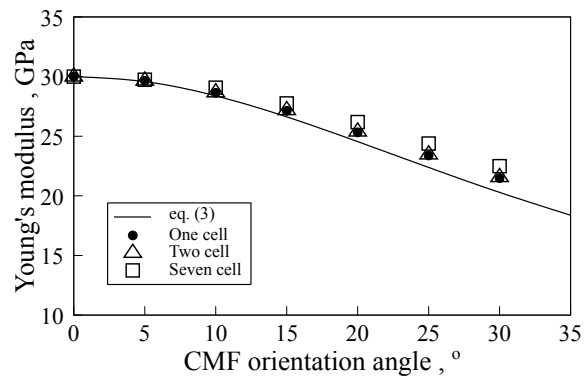


Figure 8. Young's moduli of one-, two- and seven-cells obtained in the present FE model.

anticlockwise. This mechanism is estimated to be closely related with cell torsional structure [13].

It is reported that Young's modulus of natural fibers tends to be a large statistical variation [14]. Such a statistical property was explained in terms of variation in MFA [15]. Thus, we introduced a random CMF orientation to each layer of the one-cell model, and investigated the statistical property using Monte-Carlo method. The procedure is as follows: random numbers based on normal distribution were assigned to MFAs, but each element in a layer of the FEM mesh has the same CMF angle; the angle was changed every each layer using the random numbers. When the layers locate closely, each MFA was generated with a correlation using Cholesky decomposition. Average MFA used here was 10° , and the standard deviations used were 1.0 or 2.0° . Such simulation was repeated 100 times. The simulation results are shown in Table 3. The values in the table are all average. It is shown that variations in the angle give a low impact on Young's modulus. For example, in the case of 2.0 standard deviation, the coefficient of variation in simulated Young's modulus is reduced to approximately one twenty-fifth of that in MFA, i.e. 0.173 to 0.00659. Therefore, variation of Young's modulus is considered to depend on any other factors, such as the shape of fibre and the cellulose content. However, this influence should be discussed more deeply, including the case that the variation in MFA is also given in a same layer. On the other hand, stress was affected by variation in rotation. Figure. 9 shows the variation in stress of each layer at one-cell model. Such variation in stress is considered to affect rotation behavior, and cause variation in strength. This study should be more discussed from such a point of view. Furthermore, helical structure of the multi-cell in a fibre should also need to be considered [13].

Table 3. Simulation results using random MFA.

Standard deviation in MFA	MFA (°)	Young's modulus (GPa)
1.0	10.02 (0.0903)	28.69 (0.00346)
2.0	10.06 (0.173)	28.66 (0.00659)

The values in parentheses are coefficients of variation.

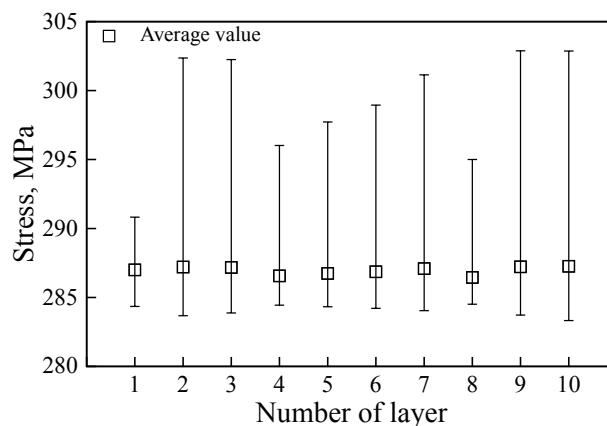


Figure 9. Stress level of each layer and variation in stress (Top and under bars are maximum and minimum values, respectively).

5. Conclusion

In this study, we confirmed the presence of rotation for a kenaf fibre, one of the representative plant-based natural fibres, during tensile loading. Fibre rotation angle was measured from motion images by a digital microscope. Result showed that the angle was correlated with Young's modulus and tensile strength to some extent. In addition, a 3D finite element model was proposed for clarification of rotation mechanism of multi-cell type natural fibres. Calculation results of the both single-cell and multi-cell models, assumed as the Z-helical structure of cellulose microfibrils (CMF), showed clockwise rotation. According to the experimental result, however, anticlockwise rotation was also confirmed. Thus, it was implied that the fibre rotation is also concerned with cell torsional structure, which could turn the fibre clockwise or anticlockwise. In addition, 3D-FEM simulation was performed by considering the variation in microfibrillar angle. As a result, rotational behavior has little influence on Young's modulus. On the other hand, variations in stress was also confirmed from the simulation results.

Acknowledgments

Funding from the Electric Technology Research Foundation of Chugoku is gratefully acknowledged.

References

- [1] JWS Hearle. The fine structure of fibers and crystalline polymers. iii. interpretation of the mechanical properties of fibers. *Journal of applied polymer science*, 7(4):1207–1223, 1963.
- [2] J. Gassan, A. Chate, and A. K Bledzki. Calculation of elastic properties of natural fibers. *Journal of materials science*, 36(15):3715–3720, 2001.

- [3] E. Marklund and J. Varna. Micromechanical modelling of wood fibre composites. *Plastics, Rubber and Composites*, 38(2-4):118–123, 2009.
- [4] A. Beakou and K. Charlet. Mechanical properties of interfaces within a flax bundle part ii: Numerical analysis. *International Journal of Adhesion and Adhesives*, 43:54–59, 2013.
- [5] V. Placet, F. Trivaudey, O. Cisse, V. Gucheret-Retel, and M Lamine Boubakar. Diameter dependence of the apparent tensile modulus of hemp fibres: A morphological, structural or ultrastructural effect? *Composites Part A: Applied Science and Manufacturing*, 43(2):275–287, 2012.
- [6] Kh M Mannan and Z. Robbany. Rotation of a natural cellulosic fibre about its fibre axis due to absorption of moisture. *Polymer*, 37(20):4639–4641, 1996.
- [7] T. Okano and Y. Nishiyama. Behavior of alkali-swollen cellulose fibers and crystal structure. *Cell. Commun.*, 2(1):2–5, 1995.
- [8] Y Nitta, K Goda, J Noda, and W-II Lee. Cross-sectional area evaluation and tensile properties of alkali-treated kenaf fibres. *Composites Part A: Applied Science and Manufacturing*, 49:132–138, 2013.
- [9] K. Tanabe, T. Matsuo, A. Gomes, K. Goda, and J. Ohgi. Strength evaluation of curaua fibers with variation in cross-sectional area. *Zairyo/Journal of the Society of Materials Science, Japan*, 57(5):454–460, 2008.
- [10] C. Baley. Analysis of the flax fibres tensile behaviour and analysis of the tensile stiffness increase. *Composites Part A: Applied Science and Manufacturing*, 33(7):939–948, 2002.
- [11] P. Xu and H. Liu. Models of microfibril elastic modulus parallel to the cell axis. *Wood science and technology*, 38(5):363–374, 2004.
- [12] C. Sellén and P. Isaksson. A mechanical model for dimensional instability in moisture-sensitive fiber networks. *Journal of Composite Materials*, 48(3):277–289, 2014.
- [13] K. Goda and Y. Nitta. Rotation of a multi-cell structure natural fiber during tensile loading - experimental validation and theoretical consideration by using a kenaf fiber - . *Sen'i Gakkaishi*, 70(10):240–247, 2014.
- [14] S. Thomas and L. A. Pothan. *Natural fiber reinforced polymer composites*. Old city publishing, 2009.
- [15] K Charlet, S Eve, JP Jernot, M Gomina, and J Breard. Tensile deformation of a flax fiber. *Procedia Engineering*, 1(1):233–236, 2009.